Iranian Journal of Geophysics, Vol 15 No 4, 2022, Page 139 – 152 (Research Article)
DOI: 10.30499/IJG.2021.266926.1312

Study of VLF radio sounding for the Ionospheric remote sensing

Alireza Mahmoudian[1*], Maryam Fallahrad [2] and Mansoure Montahaei [3]

[1] *Assistant Professor, Space Physics Department, Institute of Geophysics, University of Tehran, Iran*
[2] *M.Sc student, Space Physics Department, Institute of Geophysics, University of Tehran, Iran*
[3] *Assistant Professor, Space Physics Department, Institute of Geophysics, University of Tehran, Iran*

(Received: 11 January 2021, Accepted: 04 September 2021)

Abstract

This paper presents the recent advances made in Iran using the radio wave technique for ionospheric studies. The characteristics of the VLF signal transmitted from Turkey (26.7 kHz) and India (18.2 kHz) and received in Tehran are studied in detail to verify the behavior of signal and implement that for earthquake prediction and ionospheric remote sensing purposes. While several theories are proposed regarding the propagation of VLF, this paper aims to investigate the received signal along with the electron density variation and magnetic field strength along the propagation path. The observational data for 40 days is averaged over 24 hours with a 1-minute time resolution. The propagation of the VLF signal in the earth-ionosphere waveguide is studied by considering the electron density variation along the propagation path at several selected locations using the IRI (International Reference Ionosphere) model throughout the day. The IGRF (International Geomagnetic Reference Field) model is used to study the earth's magnetic field and the associated conductivities in the ionosphere. The excitation of secondary VLF waves in the lower ionospheric E region and propagation along the maximum conductivity is compared with the reflection from the ionosphere and propagation in the earth-ionosphere waveguide as the two different propagation mechanisms for the VLF signal. A conclusion on the propagation characteristic of the signal is made and several variation characteristics of the radio signal during the day are determined.

Keywords: VLF radio signal, ionospheric conductivity, ionospheric remote sensing

[*] Corresponding author: a.mahmoudian@ut.ac.ir

1 Introduction

The electromagnetic signal propagated through the perturbed ionosphere due to pre-seismic activity can be modulated and reveal anomalies. The ionization of the air molecules forms close to the surface due to increased radon gas emanation in the earthquake (EQ) region. While the created ions are very light, they impact the air conductivity. Initially, the ions are light and cause an increase in air conductivity. Due to ion hydration and absorption of water vapor in the lower atmosphere, the ions become larger and heavier. This process leads to less motion of created aerosol particles and a reduction in the air conductivity. Two cases may result from the above-mentioned activities. While the ions are at the early stage of formation and as a result of increased air conductivity, the potential between the ionosphere and earth is reduced. As the ion aging process begins, the ions become larger and turn into aerosol particles. Due to the low mobility of such heavy particles, the potential difference between the earth and the ionosphere will be increased. The ionosphere above the earthquake region will adjust itself to compensate for the reduced and increased potential. As the light electrons start to move around, they drag along the ions. Therefore, the ionospheric perturbation above the EQ epicenter can change the radio signal characteristics as they propagate through this region (Pulinets and Boyarchuk, 2004; Pulinets and Ouzounov, 2011).

The study of perturbations associated with the VLF radio transmission close to the epicenter of the earthquake has shown promising anomalies that could be incorporated in the EQ prediction. The termination time (TT) known as the minima in amplitude and phase of the received signal is used as the main feature in the VLF signal characteristics in such studies. TTs move gradually with changes in seasons and times (Ries, 1967; Clilverd et al., 1999). According to Kumar et al. (2013) research based on the 2006 Sumatra earthquake, the maximum deviation of TTs was reported for about 5 minutes. They also observed the effect of sunrise was delayed about 20 minute from 4 days before to 4 days after the earthquake. There is a regular deviation in the TTs for the East-West propagation path but it is more complex for the North-South path (Maekawa and Hayakawa, 2006). It should be noted that any variation in ionospheric conditions in sunrise and sunset causes the reflection height of the VLF at earth-ionosphere waveguide changes during a day (Maekawa and Hayakawa, 2006). The night reflection height decreases more than the daily reflection height (Kumar et al., 2008). Another method to investigate the anomalies associated with VLF sounding close to the EQ epicenter is nighttime fluctuation (NF). The decrease in the trend and increases in the dispersion and nighttime fluctuation are reported by Hayakawa et al. (2011). In summary, Kumar et al. (2013) reported these anomalies for 3 days before and 3 days after the mainshock. Maekawa and Hayakawa (2006) reported them within 2-6 days prior to the event. Kasahara et al. (2008) reported 5 days and Hayakawa et al. (2010) reported 5 days for trend, 3 days for dispersion and 6 days for nighttime fluctuation. Moreover, according to the data analysis of Kumar et al. (2013), only earthquakes that occur in a shallow depth and close to the TRGCP (Transmitter-Receiver Great Circle Path), affect the VLF wave propagation.

Recently, Mahmoudian and Kalaee (2019) studied the penetration of radio waves into the lower E region of the ionosphere and their propagation in this channel. This study has shown that the penetration of radio waves and exciting secondary currents in the ionosphere are reduced significantly as the transmission frequency increases from the ELF to the VLF band. While the propagation of the

VLF signal is limited in the ionospheric channel, it is still possible. The ionospheric density profile and its associated effects on the propagation of the VLF signal show the direct link between the signal anomaly and ionospheric perturbation (Mahmoudian and Kalaee, 2019).

The present paper is organized as follows. The observed VLF data from Turkey (37.24°N, 27.19°E) transmitter (TBB) operating at 26.7 kHz and INSKattabomman transmitter (VTX3) in India (8.23°N, 77.45°E) operating at 18.2 kHz over 40 days is presented. Next, the ionospheric density along the propagation path of the VLF radio signal is examined at several locations on the TRGCP. The ionospheric conductivities, including Hall, Parallel, and Pedersen are investigated to study the possibility of the VLF penetration in the lower ionosphere and propagation in the ionospheric channel. Finally, a summary and conclusion, including comparing the computed electron density profiles and ionospheric conductivities are provided.

2 Observational results

The received data from two VLF transmitters around Iran is used in this study. The VLF sounding using the Denizkoy transmitter in Turkey (37.24°N, 27.19°E) operating at 26.7 kHz and INSKattabomman in India (8.23°N, 77.45° E) operating at 18.2 kHz, and receiving station in Tehran (35.44°N, 51.23°E) are employed in this research. The receiver has two separate antennas for VLF (~15-50 kHz) and LF (~100-300 kHz). The receiver made by Elettronica Company used in the Institute of Geophysics of Tehran University is capable of detecting ten signals in the VLF and LF bands simultaneously. Figs. 1-a and 1-b show an approximate TRGCP in the India-Tehran and Turkey-Tehran propagation paths. To characterize the propagation mechanism of the radio signal, the TRGCP has been divided into 8 and 5 points along the India and Turkey paths to Tehran with approximately equal distances, respectively.

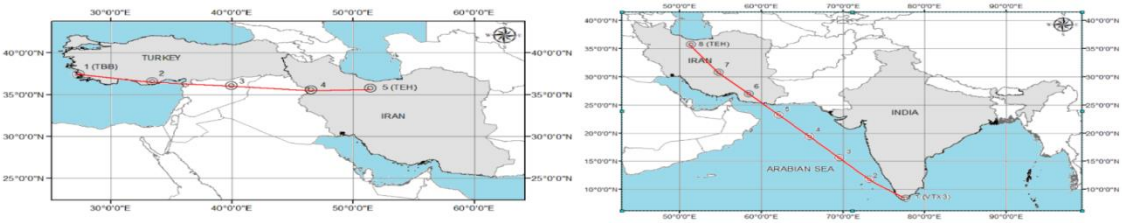

Fig 1. The geographical location of the two VLF transmitters in a) Turkey and b) India, and the receiver position in Iran. The 5 and 8 stations along with the TRGCP corresponding to Turkey-Tehran and India-Tehran paths are selected, respectively, to compare the behavior of the radio signal with ionospheric plasma density and conductivities along the propagation path.

Forty days of the recorded data from August 14, 2019, to September 23, 2019, are used in this study (Fig. 2). The averaged data over the 40 days of study associated with the VLF transmitter in India operating at 18.2 kHz is shown in Fig. 2-a. A similar result for the VLF sounding in the Turkey-Tehran path is shown in Fig. 2-b. The diurnal variation of the VLF radio signal associated with the 40 days of study for India and Turkey are shown in Figs. 2-c and 2-d, respectively. As can be seen in Figs. 2-a and 2-b, the variation of the radio signal during the day has been divided into 5 time periods:

1) Region 1 in both VLF sounding cases associated with India and Turkey transmitters corresponding to the daytime before the sunrise shows a steady signal amplitude. According to Figs. 2-a and 2-b, the constant amplitude before the sunrise lasts 3 and 3.5 hours for the India-

Tehran and Turkey-Tehran paths, respectively. This means that there is no place along the propagation path of the signal with sunlight that could enhance the ionization in the ionosphere.

2) Region 2 denotes the slow increase in the background electron density during sunrise including the lower ionosphere formation. The correlation of the slow drop in the signal amplitude as the electron density being accumulated in the ionosphere will be investigated using both propagations in the earth-ionosphere as well as in the E region along with ionospheric conductivities.

3) Region 3: As the electron density along the TRGCP reaches the maximum amplitude, the transmitted VLF signal approaches a steady-state with the lowest amplitude. The described feature is seen in the India-Tehran and Turkey-Tehran path between 7-13 UT and 7-14 UT with 10 dB and 9 dB drop in the signal strength, respectively.

4) Region 4 corresponds to the slow recovery of the radio signal amplitude as a result of decreasing ionospheric density during the sunset period. This phase of variation in signal amplitude extends for 3 hours and 2 hours in the India and Turkey-Tehran TRGCP, respectively.

5) Region 5 shows the steady VLF amplitude during the nighttime condition with reduced electron density along the propagation path.

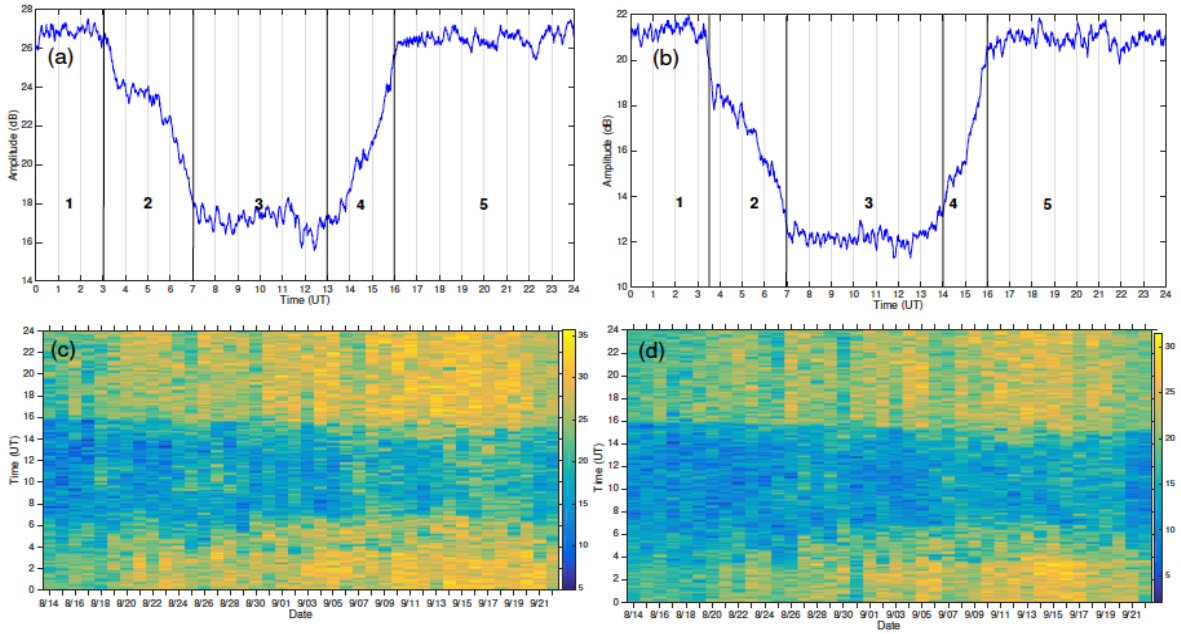

Fig 2. 40-day averaged of the VLF radio sounding in a) Turkey-Tehran and b) India-Tehran paths at 26.7 kHz and 18.2 kHz, respectively (top panels). c, d) Diurnal variation of 26.7 kHz and 18.2 kHz over 40 days of study.

Considering the sensitivity of the EQ prediction using the radio techniques to the accuracy of the received signal, including amplitude, timing and phase, the present study aims to better understand and characterize the VLF sounding data in Iran. In order to analyze the VLF data and validate the accuracy of the receiver, the first part of the paper is dedicated to the study of the ionospheric density along the signal propagation path using the IRI model. Specifically, the correspondence of the VLF signal strength received in Tehran station with the electron density variation along the propagation path, the consistency of the sunset and sunrise termination time (TT) (sharp variation in the signal amplitude), and the detection

of anomalous ionospheric density associated with the EQ located in the Fresnel zone of the propagating signal are the main objectives of the following section.

3 IRI modeling of ionospheric density along the TRGCP

The electron density along with TRGCP corresponding to the two studied paths is derived from the IRI model. The electron density altitude profile in the range of 80-140 km as well as 80-500 km is studied in order to validate the diurnal time variation of the sounded VLF signals. The electron density variation at the selected station over the propagation path of the VLF signal is determined using the IRI model. Figs. 3-a and 3-b show the averaged electron density in the altitude range of 80 to 500 km corresponding to the India and Turkey transmitters, respectively. The results show a similar time variation with the temporal evolution of the VLF signal shown in Fig 2.

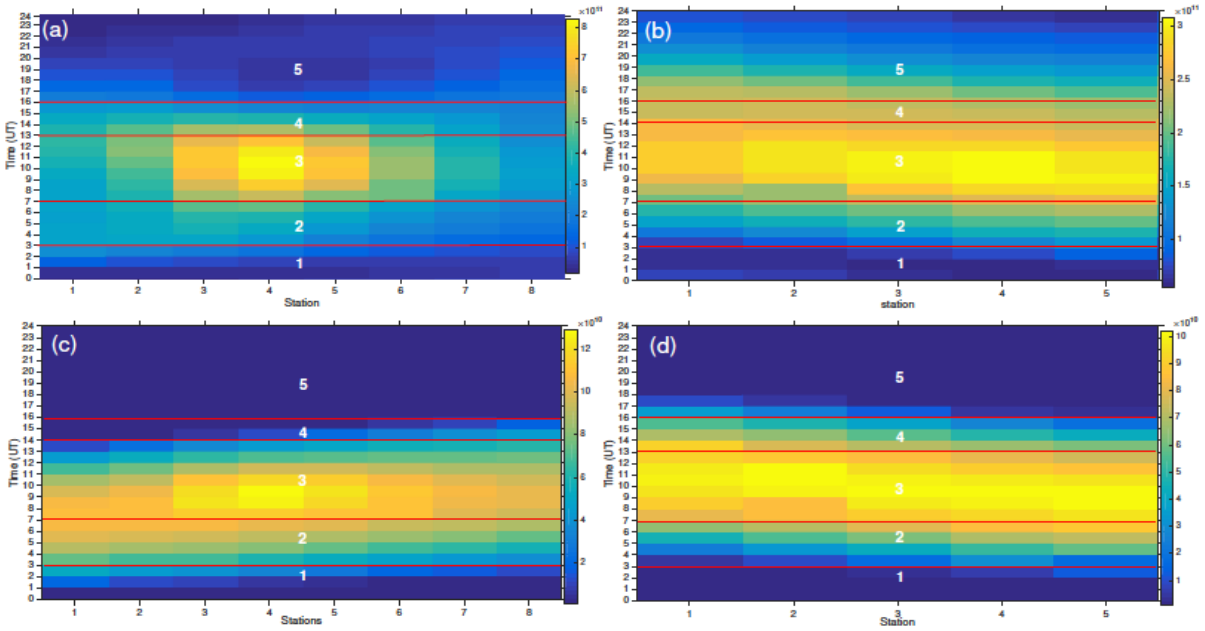

Fig 3. Averaged electron density versus daytime along the TRGCP of a, c) Turkey-Tehran and b, d) India-Tehran in the altitude range of a, b) 80-500 km and c, d) 80-140 km. The regions corresponding to the temporal evolution of the observed radio signal in Figure 2 is shown with number 1-5.

It should be noted that the first point in each figure denotes the plasma density at the transmitter location and the last point corresponds to the receiver location in Tehran. The figure has a one-hour time resolution. Specifically, the similar regions in the characterized radio signal are observed. Region 1 denotes low ionospheric density, especially in the lower region, which agrees with the maximum and constant amplitude of the radio signal. In other words, considering the radio wave propagation in the earth-ionosphere waveguide and in the absence of a lower ionospheric region will go through less reflection and as a result, a stronger signal at the receiver is expected. As the lower ionosphere starts to form during sunrise, a slow increase of electron density over the signal path occurs around 3:00 UT and continues until 7:00 UT. One unique feature in the ionospheric densities that is consistent with the observations is the electron density at earlier times in the India-Tehran path relative to the Turkey-Tehran. After 7:00 UT, the density reaches its maximum almost at every point along the TRGCP. This requires

enhanced reflection in the earth-ionosphere channel that results in a weaker received radio signal. This is in agreement with the time period 3 shown in Figs. 2-a and 2-b with minimum amplitude. The timing of the observations and the IRI model matches well. It should be noted that the maximum electron density in the India-Tehran path in Fig. 3-a is limited to 8×10^{11} m^{-3} in order to show the evident variation of ionospheric density at different stations and times clearly.

Fig. 4 shows the accumulated electron density along the signal path for India (a and c) and Turkey (b and d) transmitters. The top figures show the results of accumulated densities in the altitude range of 80 to 500 km and the bottom panels are associated with 80 to 140 km (Gołkowski et al., 2021). Another clear sign that can be inferred from the results is the formation of enhanced electron density in region 2 of Fig. 4-a that coincides with the plateau in Fig. 2-a (region 2). This is mainly due to the fact that instead of a slow increase in the electron density formation, slow delay results in the formation of a plateau in the VLF data. Such an effect cannot be seen for the Turkey transmitters as it shows a slow decay in the signal amplitude (region 2 in Fig. 2-b) associated with a smooth increase in the background electron density. Region 3 with a minimum amplitude of the measured VLF signal coincides with the maximum plasma density along the propagation path. While the electron density shows a smooth decay in region 4 for India (Fig. 3-a), a slow and plateau structure in the electron density associated with Turkey is observed in region 4 (Fig. 3-b). This is similar to the variation of the VLF curve in Figs. 2-a and 2-b. The VLF signal recovers slowly and continuously for India, but the Turkey curve shows a plateau in the recovery phase. The behavior of the density curves in region 5 and after the sunset shows a reduced electron density. As the lower ionosphere fades away, the VLF signal propagates a shorter distance and will be received at larger amplitudes.

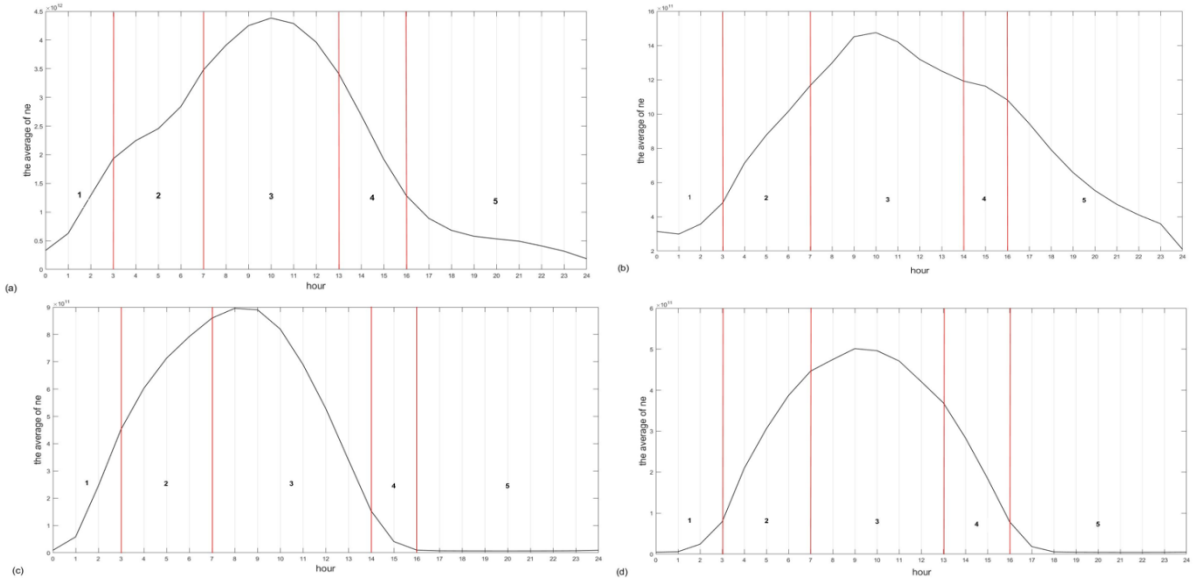

Fig 4. Summation of averaged electron density versus daytime along the TRGCP of a, c) Turkey-Tehran and b, d) India-Tehran in the altitude range of a, b) 80-500 km and c, d) 80-140 km. The regions corresponding to the temporal evolution of the observed radio signal in Figure 2 is shown with number1-5.

A similar analysis and comparison with electron density variation in the lower ionosphere, including accumulated electron density between 80 and 140 km, are shown in Figs. 4-c and 4-d. A close comparison shows a reasonable agreement with observations except that they cannot explain the plateau in regions 2 and 4 for India and Turkey, respectively.

4 Ionospheric conductivities along the TRGCP

The previous study by Mahmoudian and Kalaee (2019) showed the possibility of VLF penetration into the lower ionospheric region and propagation in the E region. According to this study, increasing the transmission frequency from the ULF to ELF and VLF band will substantially reduce the penetration height of the radio signal in the E region. The generated secondary currents in the ionosphere will act as an antenna capable of generating Helicon waves at the same frequency as the transmission frequency. It has been shown that the characteristics of the generated wave and its propagation are highly governed by the ionospheric conductivities and essentially the electron density variation. Therefore, the ionospheric density variation as a function of location along the propagation path as well as the time of the day is critical for studying such wave propagation. The increase of transmission may limit the penetration depth of the signal to the ionosphere but the generation of secondary waves in the ionosphere is feasible. In order to validate the proposed mechanism for the propagation of VLF waves, ionospheric conductivities at the selected station along the path are calculated as follows.

The parallel, Pedersen and Hall conductivities for low-frequency ELF waves with electrons and one ion species are given by Kelley and Heelis (1989):

$$\sigma_{||} = \epsilon_0 \frac{\omega_{pe}^2}{\Omega_{ce}} \quad (1)$$

$$\sigma_P = \epsilon_0 \frac{\omega_{pe}^2}{\nu_{en}} \left[\frac{\nu_{en}\Omega_{ce}}{\Omega_{ce}^2 + \nu_{en}^2} + \frac{\nu_{in}\Omega_{ci}}{\Omega_{ci}^2 + \nu_{in}^2} \right] \quad (2)$$

$$\sigma_H = \epsilon_0 \frac{\omega_{pe}^2}{\nu_{en}} \left[\frac{\Omega_{ce}^2}{\Omega_{ce}^2 + \nu_{en}^2} - \frac{\Omega_{ci}^2}{\Omega_{ci}^2 + \nu_{in}^2} \right] \quad (3)$$

where $\Omega_{ce,i}$, $\omega_{pe,i}$ and $\nu_{e,in}$ are the electron/ion gyro-frequency, plasma frequency and collision frequency with neutrals, respectively. It should be noted that for ELF waves, the ions and electrons can be considered inertialess. The Eqs. (2) and (3) are valid for the conducting fluid. The mobility of the ions at altitudes larger than 110 km leads to a cancellation of the Hall currents and decreased Hall conductivity. In the frequency range of VLF waves, ions do not have time to move, while the electrons can be considered inertialess. This leads to conductive fluid equations with immobile ions. In this case, the terms related to ions (second terms) can be neglected in Eqs. (2) and (3).

Plasma frequency, electron gyro-frequency and collision frequency with neutrals are given by:

$$\omega_{Pe} = \sqrt{\frac{n_e \times e^2}{m_e \times \varepsilon_0}} \quad \left(rad/_S\right) \quad (4)$$

$$\omega_{ce} = \frac{e \times B}{m_e} \quad \left(\mathrm{rad}/_{\mathrm{S}}\right) \quad (5)$$

$$\nu_{en} = 2.33 \times 10^{-11} n(N_2)\left(1 - 1.21 \times 10^{-4} T_e\right) T_e + 1.82 \times 10^{-10} n(O_2)\left(1 + 3.6 \times 10^{-2}\sqrt{T_e}\right)\sqrt{T_e} + 8.9 \times 10^{-11} n(O)\left(1 + 5.7 \times 10^{-4} T_e\right)\left(rad/_S\right) \quad (6)$$

where n_e is the electron density and e is the electron charge. m_e is electron mass. ε_0 is permittivity vacuum and B is magnetic field size. T_e is electron temperature and $n(N_2)$, $n(O_2)$ and $n(O)$ are neutral particle density.

Fig. 5 shows neutral particle density (N_2, O_2 and O) in the altitude range of 80-500 km. Figs. 6-a and 6-b show the magnetic field size along the Turkey-Tehran path and India-Tehran path,

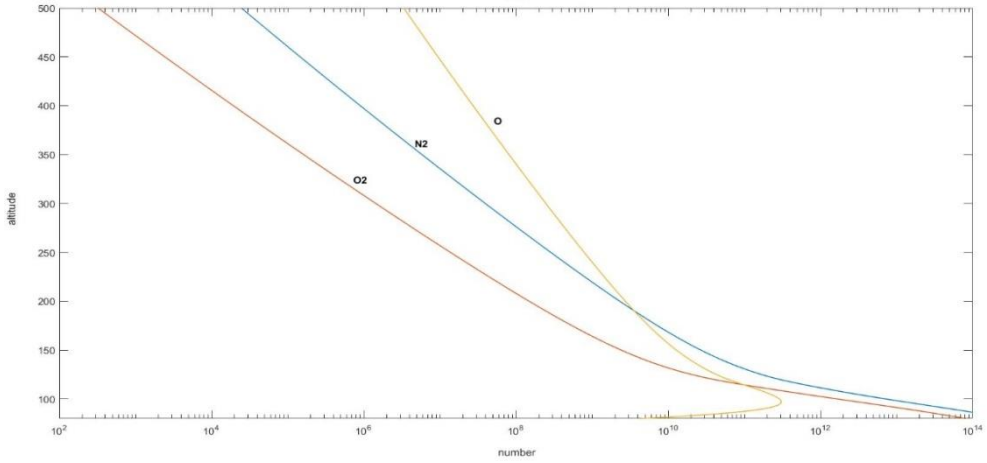

Fig 5. Neutral particle density (N_2, O_2 & O) in the altitude range of 80-500 km.

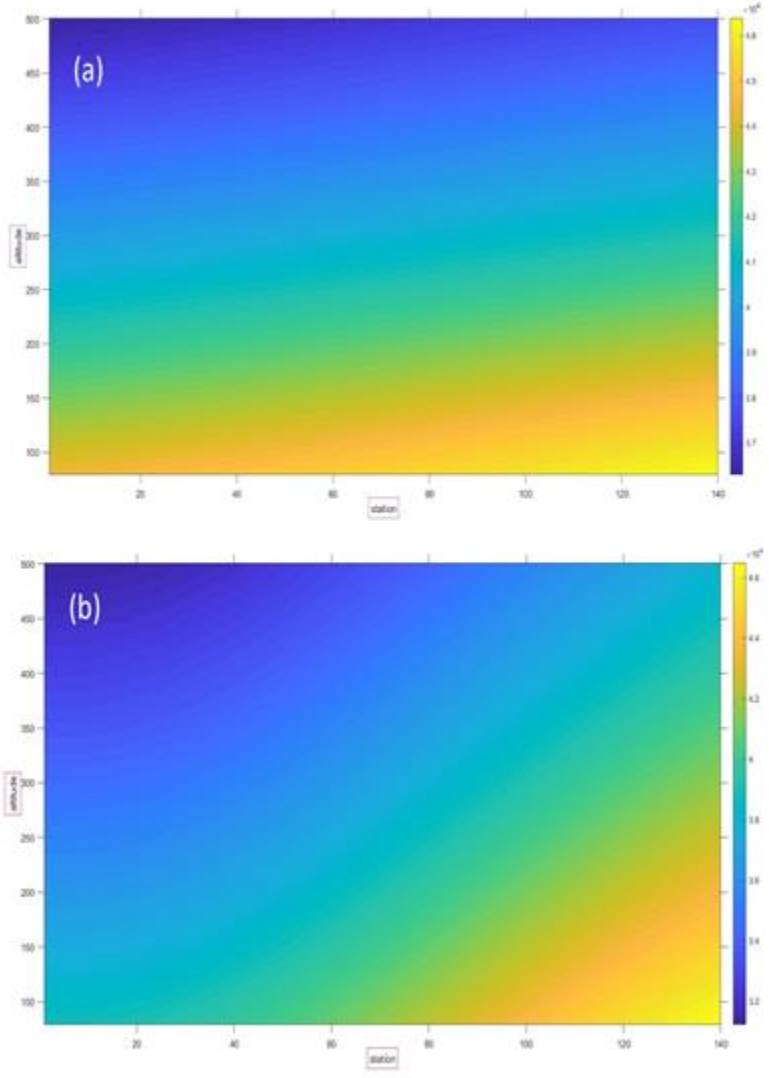

Fig 6 . The magnetic field size along a) Turkey-Tehran path b) India-Tehran path.

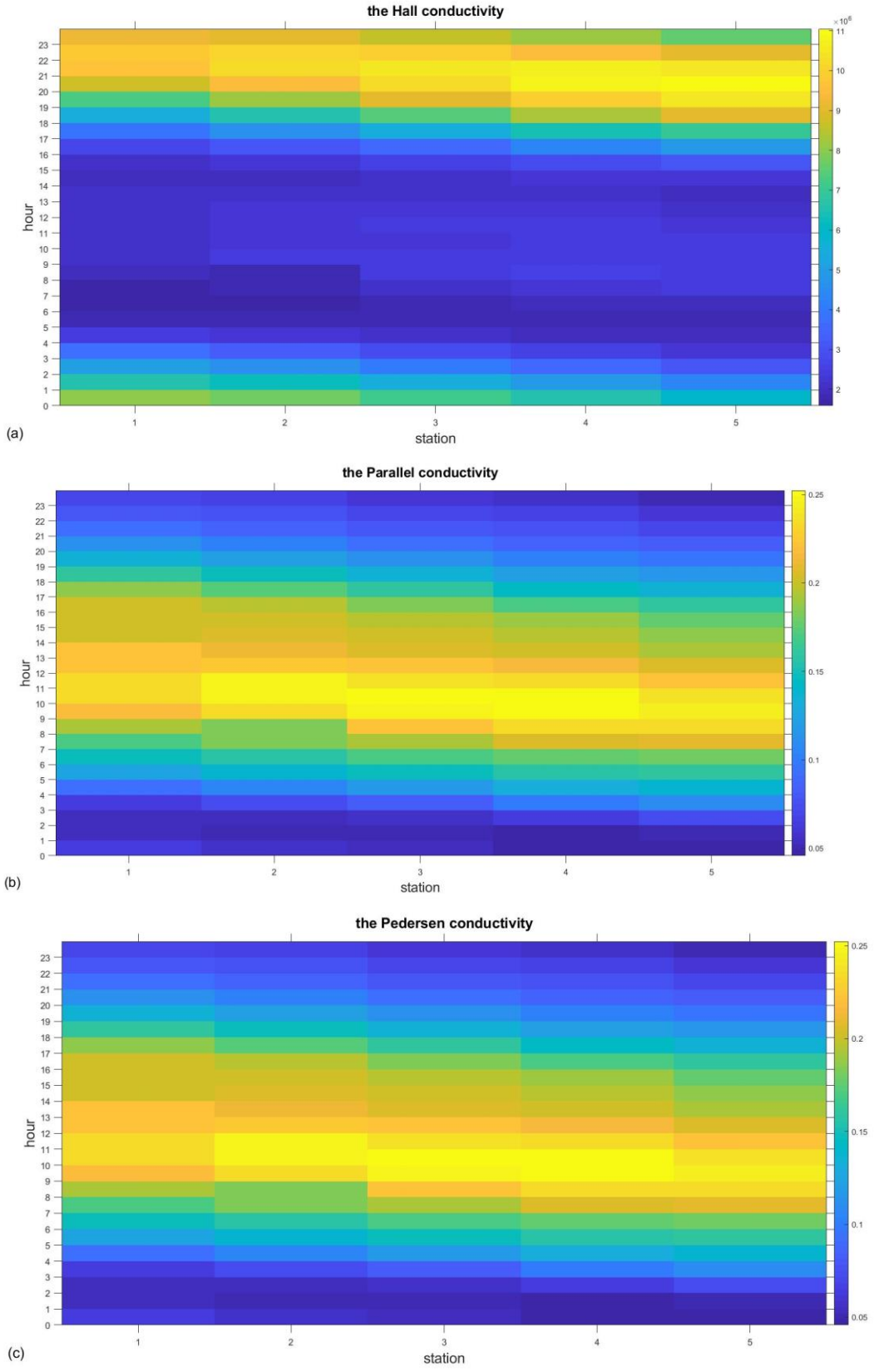

Fig 7. : Plasma frequency, electron gyro-frequency and collision frequency with neutrals including a) $\overline{\omega_{pe}}$ b) $\overline{\omega_{ce}}$ c) $\overline{\nu_{en}}$ along Turkey-Tehran path.

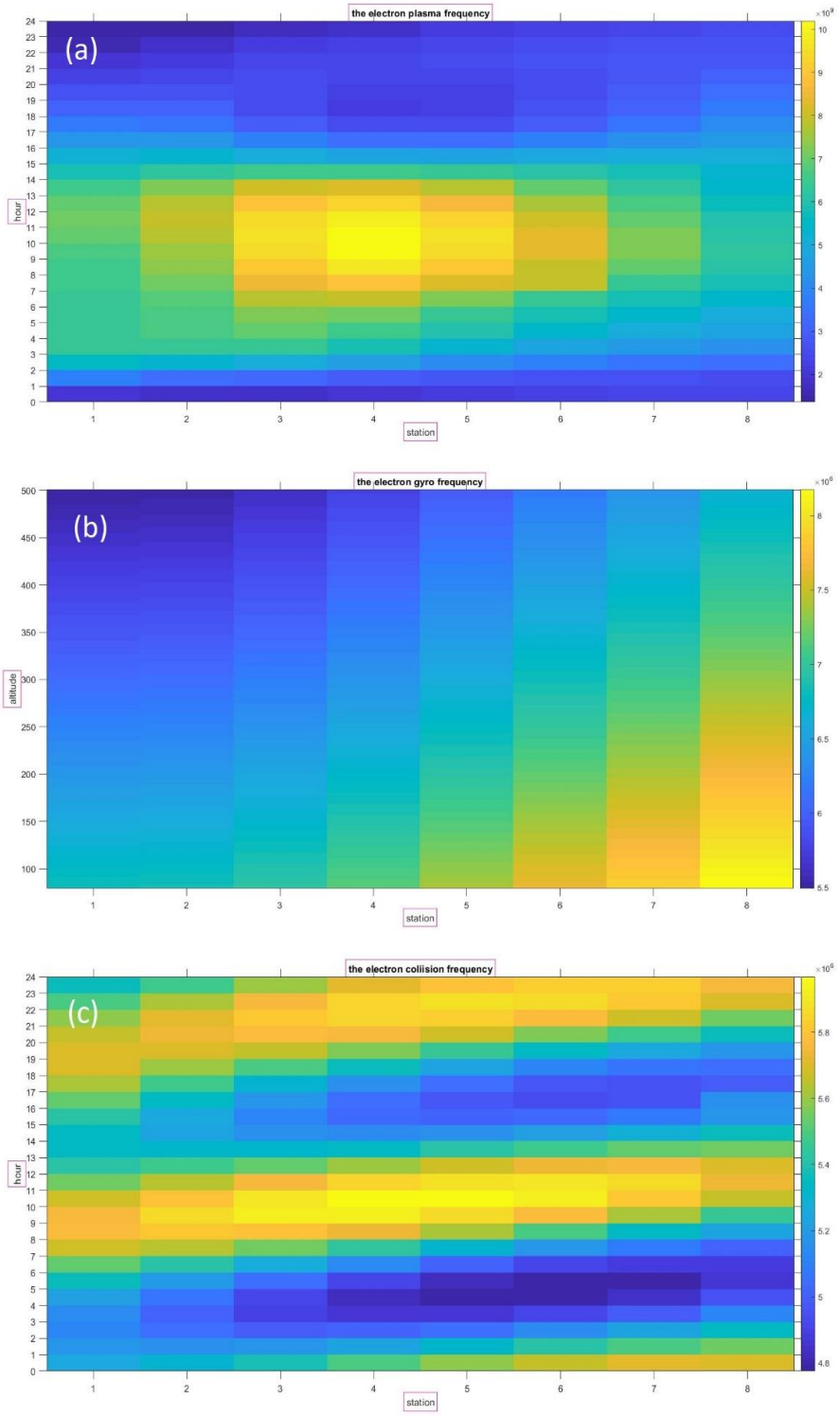

Fig 8. Plasma frequency, electron gyro-frequency and collision frequency with neutrals including a) $\overline{\omega_{p_e}}$ b) $\overline{\omega_{ce}}$ c) $\overline{\nu_{en}}$ along India-Tehran path.

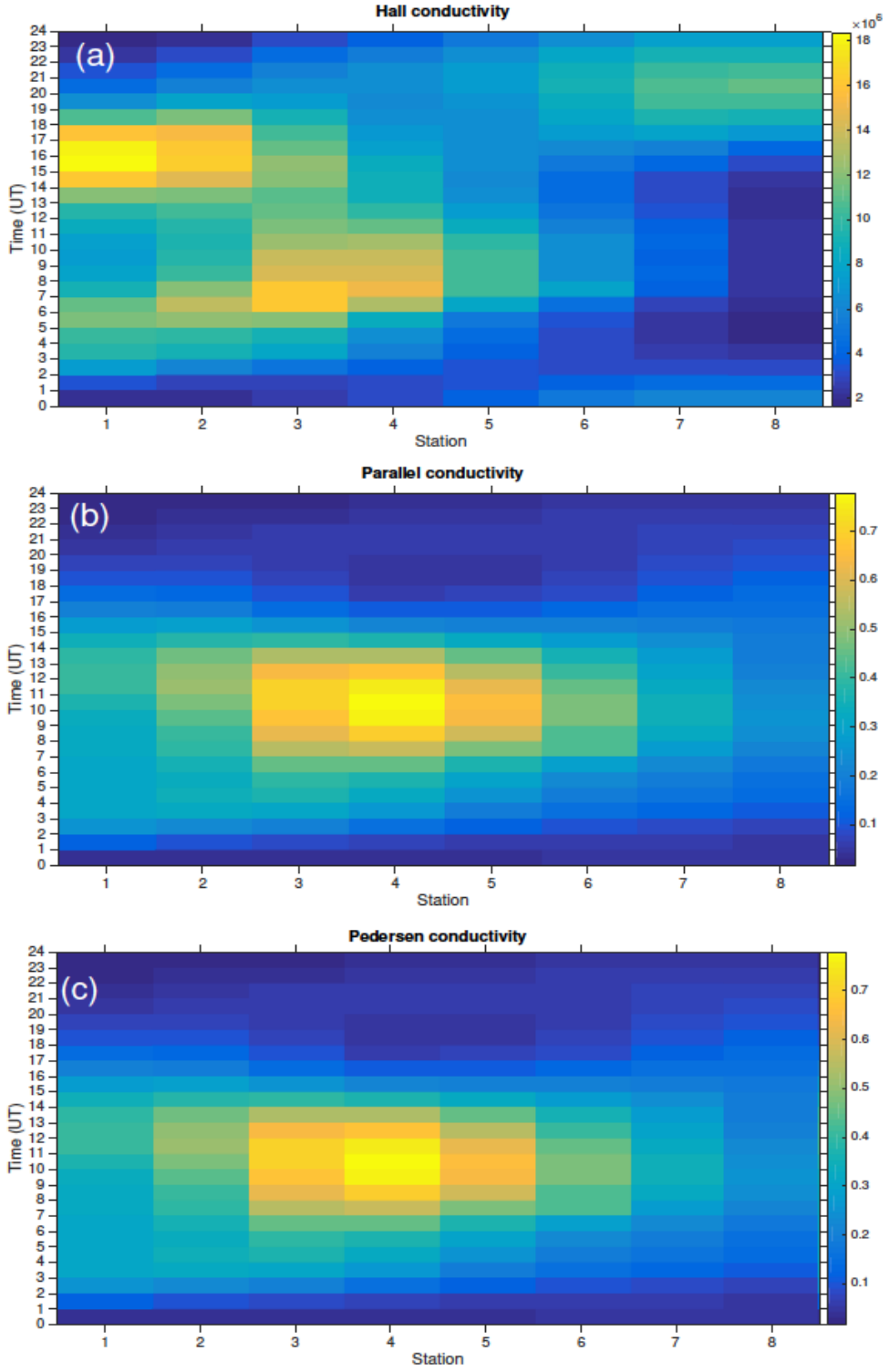

Fig 9. Corresponding ionospheric conductivities including a) Hall b) parallel c) Pedersen conductivities along Turkey-Tehran path.

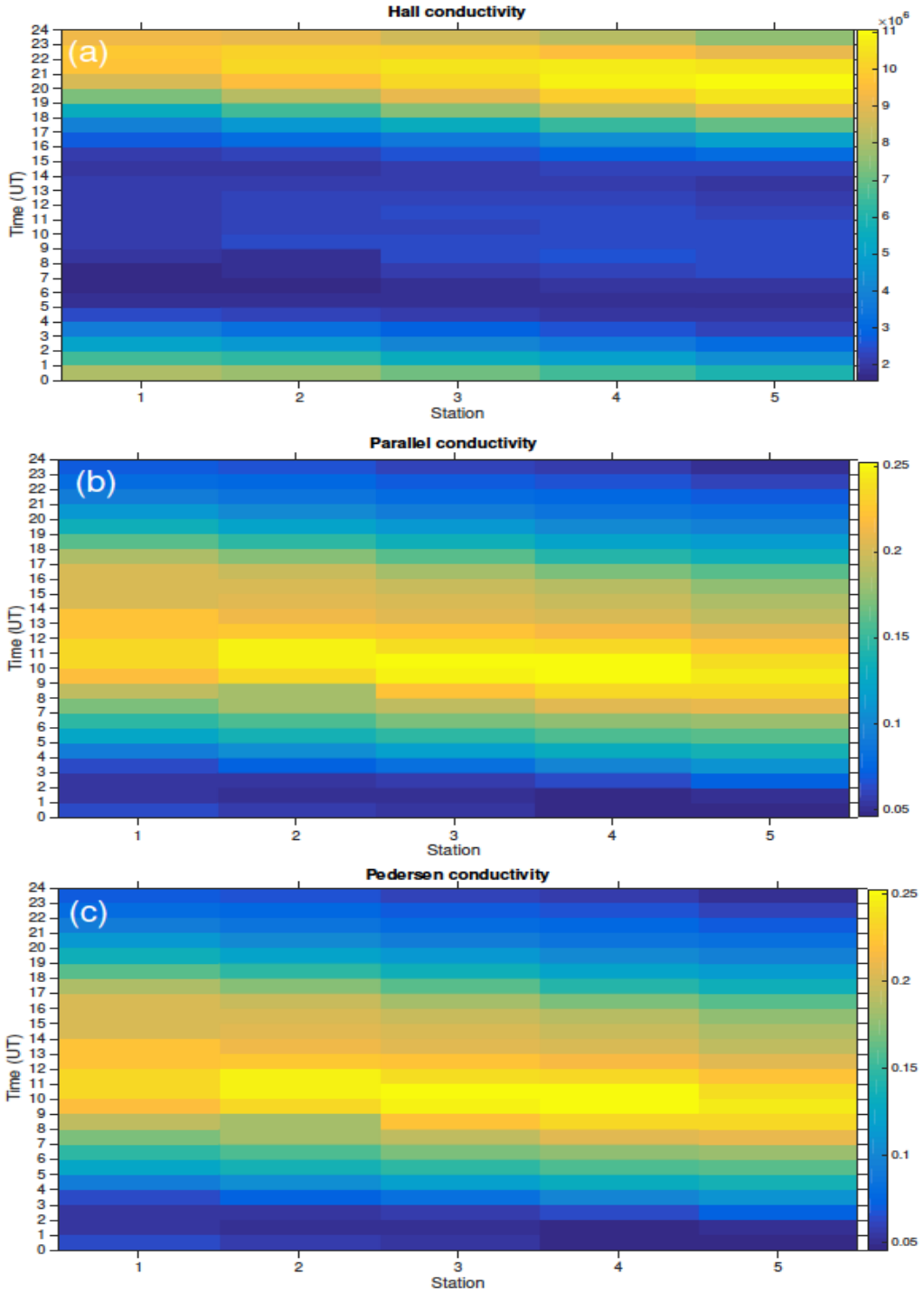

Fig 10. Corresponding ionospheric conductivities including a) Hall b) parallel c) Pedersen conductivities along India-Tehran path.

respectively. Fig. 7 shows plasma frequency, electron gyro-frequency and collision frequency with neutrals including (a) ω_{Pe}, (b) ω_{ce} and (c) ν_{en} along the Turkey-Tehran path. Fig. 8 shows the same parameters as Fig. 7, but in the India-Tehran path.

Fig. 9 shows the corresponding ionospheric conductivities including Hall (Fig. 9-a), Parallel (Fig. 9-b) and Pedersen (Fig. 9-c) conductivities along the Turkey-Tehran path. The results shown in this figure show the summation of conductivities in the altitude range of 80

to 500 km. Close comparison of the hourly variations of the maximum conductivity value with the electron density plot shown in Fig. 3-a as well as the temporal evolution of the VLF signal in Fig. 2-a show that the parallel and Pedersen conductivities can truly explain the five regions characterized in the signal daily variation. Similar results are presented in Fig. 10, showing the three components of conductivities associated with the India-Tehran path. This figure also shows a similar trend in the time evolution of parallel and Pedersen conductivities in agreement with the characteristics of the received signal. Therefore, such a comparison validates the possible penetration of the VLF signal into the lower ionospheric E region and propagation in that channel.

5 Summary and conclusion

The present paper aimed at detailed investigation and understanding of VLF radio propagation in the ionosphere with the purpose of ionospheric remote sensing. The VLF sounding from India (8.23°N, 77.45°E) and Turkey (37.24°N, 27.19°E), received in Tehran (35.44°N, 51.23°E) is studied for 40 days during 2019. The diurnal time variation of the radio signal is examined and characterized. Five distinct daily variations in the radio signal are determined. The ionospheric densities obtained from the IRI model in two altitude range of 80-140 km and 80-500 km are studied in order to determine the lower ionosphere and whole ionospheric plasma density role in the propagation of the radio signal. The plasma density and electron density refer to the same concept in the ionospheric physics (Baumjohann and Treumann, 1996). It has been demonstrated that the electron density profile in 80-500 km shows a better agreement with the temporal evolution of the radio signal. The idea of VLF penetration into the lower E region and propagation along the highly conductive channel is investigated. The Hall, Pedersen and Parallel conductivities are calculated along the TRGCP for the India and Turkey VLF transmitters. The results show a good correlation of the time variation of the conductivities throughout the day with the observed VLF data. Therefore, VLF sounding data could also be explained by propagation in the lower ionospheric channel. This study is critical to characterize the behavior of the signal and determine any anomaly produced as a result of the Lithosphere-Atmosphere-Ionosphere Coupling (LAIC) on the propagation of signal over the disturbed ionospheric regions as a result of the earthquake. Any changes in the signal structure for different months and seasons can be implemented to determine the earthquake activity on the signal propagation path.

Acknowledgments

MF was supported through a research grant at the Institute of Geophysics, University of Tehran. AM was supported by Iran National Science Foundation (INSF).

References

Baumjohann, W., and Treumann, R., 1996, Basic Space Plasma Physics (Revised Edition): Imperial College Press.

Bilitza, D., Altadill, D., Truhlik, V., Shubin, V., Galkin, I., Reinisch, B., and Huang, X., 2017, International reference ionosphere 2016: From ionospheric climate to real-time weather predictions: Space Weather, **15**, 418-429, doi:10.1002/2016SW001593.

Bilitza, D., 2018, IRI the International Standard for the Ionosphere: Advances in Radio Science, **16**, 1-11, doi 10.5194/ars-16-1-2018.

Clilverd, M. A., Thomson, N. R., and Rodger, C. J., 1999, Sunrise effects on signals propagating over a long north–south path: Radio Science, **34**, 939–948.

Gołkowski, M., Renick, C., and Cohen, M. B., 2021, Quantification of ionospheric perturbations from lightning using overlapping paths of VLF signal propagation: J. Geophys. Res., Space Physics, **126**, e2020JA028540, doi 10.1029/2020JA028540.

Hayakawa, M., Kasahara, Y., Nakamura, T, Hobara, Y., Rozhnoi, A., Solovieva, M., and Molchanov, O. A., 2010, A statistical study on the correlation between lower ionospheric perturbations as seen by subionospheric VLF/LF propagation and earthquakes: J. Geophys. Res., **115**, A09305, http://dx.doi.org/10.1029/2009JA015143.

Hayakawa, M., Raulin, J. P., Kasahara, Y., Bertoni, F. C. P., Hobara, Y., and Guevara-Day, W., 2011, Ionospheric perturbations in possible association with the 2010 Haiti earthquake, as based on medium-distance subionospheric VLF propagation data: Natural Hazards and Earth System Sciences, **11**, 513–518.

Kasahara, Y., Muto, F., Horie, T., Yoshida, M., Hayakawa, M., Ohta, K., Rozhnoi, A., Solovieva, M., and Molchanov, O. A., 2008, On the statistical correlation between the ionospheric perturbations as detected by subionospheric VLF/LF propagation anomalies and earthquakes: Natural Hazards and Earth System Sciences, **8**, 653–656, doi 10.5194/nhess-8-653-2008.

Kumar, A., Kumar, S., Hayakawa, M., and Menk, F., 2013, Subionospheric VLF perturbations observed at low latitude associated with earthquake from Indonesia region: Journal of Atmospheric and Solar-Terrestrial Physics, **102**, 71-80.

Kumar, S., Kumar, A., and Rodger, C. J., 2008, Subionospheric early VLF perturbations observed at Suva: VLF detection of red sprites in the day: J. Geophys. Res., **113**, A03311, http://dx.doi.org/10.1029/2007JA012734.

Maekawa, S., and Hayakawa, M., 2006, A statistical study on the dependence of characteristics of VLF/LF terminator: IEEE Transactions on Fundamentals and Materials, **126**(4), 220–226.

Mahmoudian, A., and Kalaee, M. J., 2019, Study of ULF-VLF wave propagation in the near-Earth environment for earthquake prediction: Advances in Space Research, **63**(12), 4015-4024.

Pulinets, S., and Boyarchuk, K., 2004, Ionospheric Precursors of Earth quakes: Springer, Berlin, Germany.

Pulinets, S., and Ouzounov, D., 2011, Lithosphere-atmosphere-ionosphere coupling (LAIC) model—A unified concept for earthquake precursor validation: Journal of Asian Earth Science, **41**, 371–382, doi:10.1016/j.jseaes.2010.03.005.

Rawer, K., Bilitza, D., and Ramakrishnan, S., 1978, Goals and status of the international reference ionosphere: Review of Geophysics, **16**, 177-181.

Ries, G., 1967, Results concerning the sunrise effect of VLF signals propagated over long paths: Radio Science, **2**, 531–538.